Geomechanics and Engineering, *Vol. 32, No. 4 (2023) 427-443*
https://doi.org/10.12989/gae.2023.32.4.427

Investigation of effects of twin excavations effects on stability of a 20-storey building in sand: 3D finite element approach

Hemu Karira[1], Dildar Ali Mangnejo*[1], Aneel Kumar[2], Tauha Hussain Ali[2] and Syed Naveed Raza Shah[1]

[1]*Department of Civil Engineering, Mehran University of Engineering and Technology, Shaheed Zulfiqar Ali Bhutto Campus, Khairpur Mir's, Sindh, Pakistan*
[2]*Department of Civil Engineering, Mehran University of Engineering and Technology, Jamshoro, Sindh, Pakistan*

(*Received November 27, 2022, Revised January 11, 2023, Accepted January 29, 2023*)

Abstract. Across the globe, rapid urbanization demands the construction of basements for car parking and sub way station within the vicinity of high-rise buildings supported on piled raft foundations. As a consequence, ground movements caused by such excavations could interfere with the serviceability of the building and the piled raft as well. Hence, the prediction of the building responses to the adjacent excavations is of utmost importance. This study used three-dimensional numerical modelling to capture the effects of twin excavations (final depth of each excavation, H_e=24 m) on a 20-storey building resting on (4×4) piled raft. Because the considered structure, pile foundation, and soil deposit are three-dimensional in nature, the adopted three-dimensional numerical modelling can provide a more realistic simulation to capture responses of the system. The hypoplastic constitutive model was used to capture soil behaviour. The concrete damaged plasticity (CDP) model was used to capture the cracking behaviour in the concrete beams, columns and piles. The computed results revealed that the first excavation- induced substantial differential settlement (i.e., tilting) in the adjacent high-rise building while second excavation caused the building tilt back with smaller rate. As a result, the building remains tilted towards the first excavation with final value of tilting of 0.28%. Consequently, the most severe tensile cracking damage at the bottom of two middle columns. At the end of twin excavations, the building load resisted by the raft reduced to half of that the load before the excavations. The reduced load transferred to the piles resulting in increment of the axial load along the entire length of piles.

Keywords: damage; differential settlement; high-rise building; piled raft; twin excavations

1. Introduction

Normally, Urban development in densely environmental areas often involves the construction of underground space (e.g., a basement). Multi-propped excavations are widely utilized for basement construction of the buildings and development of underground structures such as metro stations and cut-and-cover tunnels that are close to the existing foundation of adjacent structures, i.e., high-rise buildings, flyovers, and elevated trains (Fang *et al.* 2022, Hemu *et al*. 2022, Soomro *et al.* 2022, Shi *et al.* 2019).

When existing structures are supported by pile foundations, a suitable evaluation of the responses of existing piles cause by the adjacent excavation is imperative to ensure the stability and integrity of both the structures and piles (Ding *et al.* 2017, Ng *et al.* 2021, Qian *et al.* 2020). Besides, they have to be still fully functional without changing the way they respond to the loads. Several previous studies (e.g., Finno *et al.* 1991, Goh *et al.* 2003, Kroff *et al.* 2016, Ng *et al.* 2021) revealed that the basement excavations for new structures would unavoidably induce an excessive soil movement behind the retaining wall system and consequently, the soil movements can cause an additional lateral loading on nearby existing pile foundation, resulting in an augmentative bending moment and deflection on piles which may result to structural distress or even failure. Therefore, the possibility of causing risk to nearby pile structures is one of the main design concerns in such projects. To this end, a reasonable evaluation is essential for preventing or minimizing the damage to adjacent piles. A large number of previous publications (using analytical and numerical methods) have revealed that the existing piles can be affected by the horizontal soil movements owing to nearby excavation activities (Lee 2019, Liyanapathirana and Nishanthan 2016, Zhang *et al.* 2011, Mu *et al.* 2021). Based on these past studies, they found that an extra bending moment and deflection within the existing piles adjacent to excavations were significantly influenced by numerous factors, i.e., excavation depth and width, retaining wall stiffness, supporting system stiffness and spacing, diameter and length of pile, location of pile away from the excavation face, fixity conditions of pile head, and undrained shear strength of soil layer. Therefore, it is imperative to assess the pile responses for maintaining the serviceability of existing structures. Liyanapathirana and Nishanthan (2016) and Zhang *et al.* (2011) analysed the excavation-induced pile behaviour using the finite element method and the centrifuge test. In terms of influence parameters of excavation construction. Boone *et al.* (1999) provided a modified approach for estimating potential damage and

*Corresponding author, Ph.D. Student
E-mail: dildarali@muetkhp.edu.pk

ISSN: 2005-307X (Print), 2092-6219 (Online)

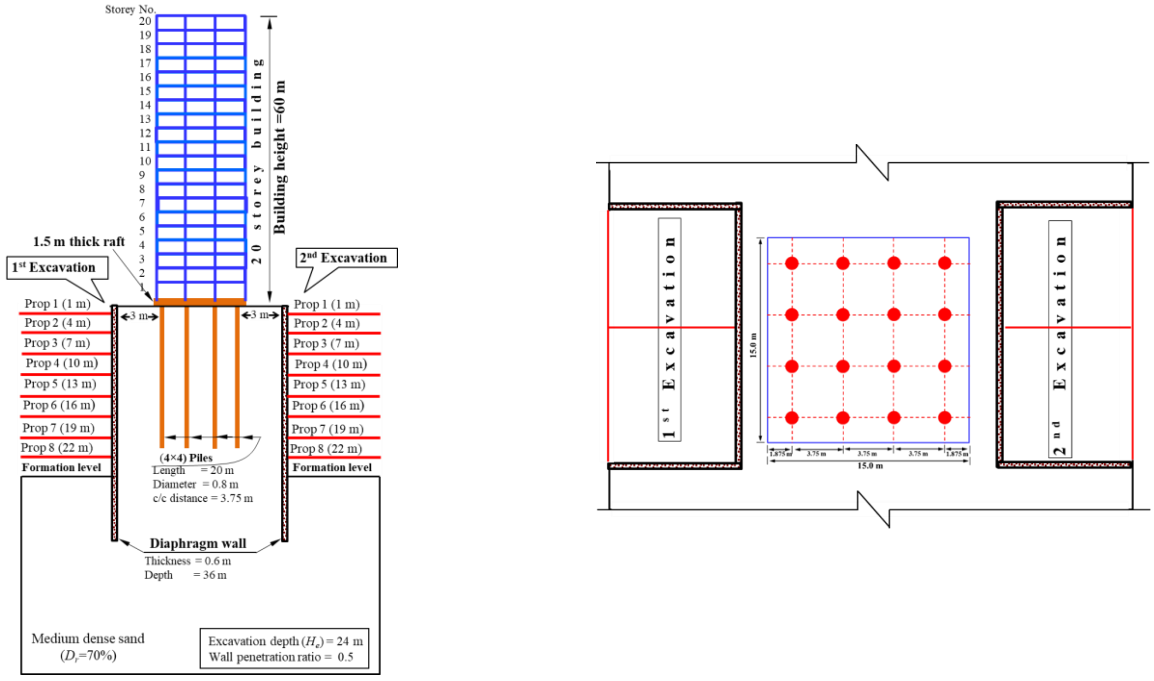

(a) Elevation view (b) Plan view

Fig. 1 General setup of the high-rise building and a basement (a) Elevation view and (b) plan view

compared to case histories using construction data from a large braced excavation. Hsiao *et al.* (2008) considered the calculated settlement as the load in the context of reliability analysis and proposed a simplified model for evaluating the damage potential of a building adjacent to a braced excavation. Long (2001) summarized the general trends and patterns based on some 300 case histories of wall and ground movements due to deep excavations worldwide. Among those numerical studies, however, responses of framed building to excavation were reported in a limited number of studies. However, most of the previous studies have focused on the effects of excavation effects on pile foundations. Therefore, there is a gap of systematic research on the responses of a high-rise building subjected to live load and resting on piled raft to advancement of adjacent excavation. Moreover, the development of underground transportation systems often involves twin excavations, which are sometimes unavoidably constructed adjacent to existing buildings. It is widely known that the highly nonlinear stress-strain characteristic of soils greatly depends on the stress path, stress level, and strain level (Atkinson *et al.* 1990) and soil stiffness that can change with the strain variations even at low strain levels. Regarding twin excavations, the displacement characteristic is governed by the stress path in turn depends on stress history and stress state (Hong *et al.* 2015). Therefore, it is vital to investigate a high-rise building response not only to first excavation but also subsequent excavation in sand. To obtain a satisfactory numerical model of twin excavations effects on high-rise building, the analysis needs to take account of the small strain non-linearity of soil. In view of the aforementioned issues, this study aims at systematically investigating the settlement and load transfer mechanism of an existing 20-storey high rise building due to twin excavations (which were carried out on the either side of the building) in sand. To achieve these objectives, a three-dimensional finite element analysis was conducted. The building deformation (i.e., differential settlement, deflection and inter-storey drift) and piled raft (i.e., induced bending moment and shear forces in the piles) were presented and discussed.

2. Characteristics of a soil-pile-structure system

2.1 General

With the prime objective of investigating twin excavations building interaction, three-dimensional finite element analyses were adopted in this study. Twin excavations (which were carried out on the either side of the building) carried out in the close proximity of a 20-storey high rising building which is resting on a (4×4) piled raft foundation in sand (with relative density, Dr=70%). Fig. 1(a) illustrates the general setup of the 20-storey building founded on piled raft and a basement. In practice, the final excavation depth of basement commonly varied from 12 to 30 m, and the thickness of retaining wall varied from 0.3 to 1.0 m (Ng *et al.* 2017, Shi *et al.* 2022a). To simulate an actual construction in practice, the final depth excavation (H_e) of 24 m and a wall thickness of 0.6 m was simulated in this study. Each excavation was carried out in eight stages (with depth of each stage = 3 m). The ratio of wall penetration depth to excavation depth is typically 0.5-2 in engineering practice (Hong *et al.* 2015) and thus a value of 0.5 is adopted in this study. The retaining wall was supported by eight levels of props with vertical spacing of

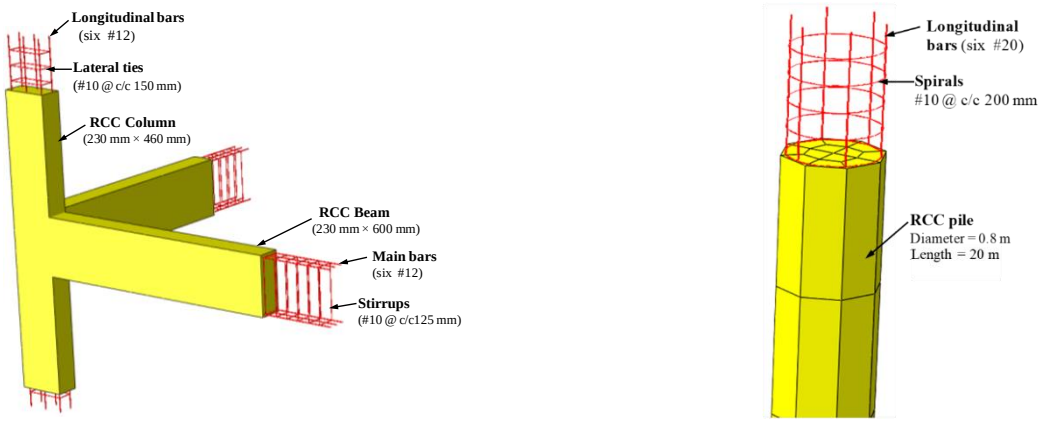

(a) Beams and columns (b) a typical pile

Fig. 2 Sections and reinforcement details of (a) beams and columns and (b) a typical pile

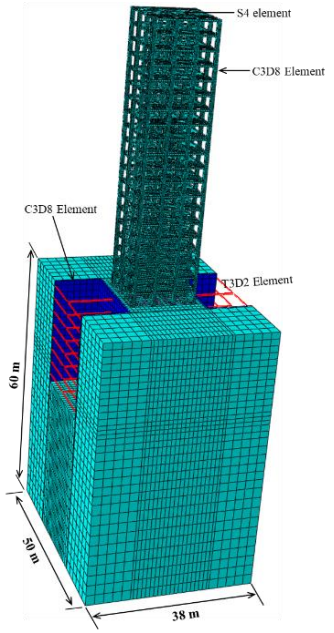

Fig. 3 3D finite element mesh (showing model of the high-rise building and twin excavations systems)

3.0 m. The first level of props was installed at 1.0 m below the ground surface. The props are modelled as soft with axial rigidity of 81 × 10^3 kNm (Shi *et al*. 2019). A 60-m high, 15-m wide 20-storey, concrete building with three spans in each direction was selected in study. The 20-storey building is founded on piled raft (details are given in section). The clear distance between the closest pile and the diaphragm wall was 3.0 m (3.75dp). Since the prime objective of this parametric study is to assess the impact of twin excavations on the 20-storey building under working condition. The live load of 5 kPa (Standard Australia 2002) was adopted in this study.

2.2 Features of the building

Fig. 2(a) shows the sections (with reinforcement details) of a typical beam and column of the high-rise building, respectively. The sections by conducting a routine design procedure by conducting analysis and design using SAP2000 based on ASI. All the sections of beams and columns are rectangular in shape having sizes of 230 mm by 600 mm and 230 mm by 460 mm, respectively. Each beam is reinforced with tension and compression steel bars. Tension and compression reinforcement consist of three numbers of 12 mm diameter bars and three numbers of 12 mm diameter bars, respectively. The bars are places at centre-to-centre spacing of 60 mm. These main bars are confined by the stirrups of diameter 10 mm at centre to centre spacing of 125 mm. Each column is reinforced with six numbers of 12 mm diameter main bars. These main bars are confined by the lateral ties of diameter 10 mm at centre to centre spacing of 150 mm.

2.3 Features of the foundation

The building was founded on a square raft of size 15 m and 1.5 m thick supported by a group of piles in a 4×4 configuration with centre-to-centre distance of 3.75 m (see

Table 1 Mechanical properties of concrete and steel reinforcement for frame of the building

Material	Constitutive Model	Input parameter	Magnitude
Concrete	Damage plasticity model	Mass density (kg/m^3)	2400
		Elastic Modulus (kPa)	3.15×10^7
		Poisson's ratio (ν)	0.2
		Dilation angle (^{o})	30
		Eccentricity	0.1
		Stress ratio	0.666
		Ultimate strength ratio	1.16
		Tensile yield stress (kPa)	1.32×10^3
		Compressive yield stress (kPa)	6.17×10^3
Steel reinforcement	Elastic-perfectly-plastic	Mass density (kg/m^3)	7850
		Elastic Modulus (kPa)	2000
		Poisson's ratio (ν)	0.3
		Yield stress (kPa)	4×10^5

Table 2 Elastic properties of concrete for piles and diaphragm walls

Description	Parameter
Young's Modulus, E	35 GPa
Poisson's ratio, v	0.3
Density, ρ	2400 kg/m^3

Fig. 1(b)). The diameter (d_p) and length (L_p) of each pile were 0.8 m and 20 m, respectively. Fig. 2(b) shows the section of a typical pile with reinforcement. The pile is reinforced with six numbers of 20 mm diameters longitudinal bars which are equally spaced around the pile. These bars are connected with spirals of 10 mm diameter with centre to centre spacing of 200 mm.

2.4 Characteristics of the numerical model

Fig. 3 shows the finite element mesh developed in Abaqus software . The size of the mesh numerical run was taken as 50 m × 50 m × 60 m. The different structural components of the building frame (i.e., beams and columns) and, slabs and raft were modelled by Eight-noded hexahedral brick elements (C3D8) and four-node shell elements (S4), respectively. The concrete damaged plasticity constitutive model which is improved on the basis of fracture energy theory and a plastic-damage model proposed by Lubliner *et al*. (1989) is adopted to simulate the nonlinear behaviour of the building frame. Elastic perfectly-plastic constitutive model is used to model the mechanical behaviour of steel reinforcement. The detailed steel reinforcement and concrete material properties are listed in Table 1. Eight-noded hexahedral brick elements are used to model the soil, the pile and the diaphragm wall, while two-noded truss elements are adopted to model the props. The concrete pile, the diaphragm wall and the props were assumed to be linear elastic with Young's modulus of 35 GPa and Poisson's ratio of 0.25. The unit weight of concrete was assumed to be 24 kN/m^3. The parameters for the piles and the diaphragm wall are summarised in Table 2.

Since the stress-strain relationship of soils is highly nonlinear even at very small strain and the stiffness of soil depends on the recent stress or strain history of the soil (Atkinson *et al*. 1990, Niemunis and Herle 1997), an advanced hypoplastic model was used to simulate the behaviour of sand in this study. The basic hypoplastic soil model requires eight material parameters to describe the non-linear behaviour of sand (ϕ'_c, h_s, n, e_{d0}, e_{c0}, e_{i0}, α and β). Parameter ϕ'_c is soil frictional angle at critical state. Parameters h_s and n are used to describe shape of limiting void ratio lines. Parameters e_{d0}, e_{c0} and e_{i0} are reference void ratios of isotropic normal compression line, critical state line and minimum void ratio line, respectively. Effects of soil relative density on peak frictional angle and shear stiffness are characterised by parameters of α and β. To consider the small strain stiffness and stress path-dependent soil behaviour, the concept of intergranular strain is incorporated into the basic model (Niemunis and Herle 1997), which includes additional five parameters (m_R, m_T, R, β_r and χ). By using the concept of intergranular strain, the modified hypoplastic sand model has the ability to capture effects of shear strain and stress path on soil stiffness. These five parameters were obtained by fitting the stiffness degradation curves of Toyoura sand obtained from the stress-path triaxial tests carried out by Ng *et al*. (2021). The model parameters were taken from study by Shi et al., (2022b). They calibrated and validated all the parameters of the hypoplastic sand model against their centrifuge test results (which was performed to simulate excavation in sand). These parameters are summarized in Table 3. The lateral coefficient of earth pressure (K_0) is estimated by the empirical equation ($1-\sin\varphi'$) proposed by Jáky (1944), where φ' is internal frictional of soil at the critical state. Since the internal friction angle of Toyoura sand at the critical state is 31°, thus, the K_0 value is estimated as 0.5.

2.5 Soil structure interactions and boundary conditions

While modelling excavation-pile-soil problem, one of the important aspects of modelling soil structure interaction (SSI) is to establish interaction between pile and

Table 3 Hypoplastic model parameters of sand adopted in this study

Description	Parameter
Effective angle of shearing resistance at critical state: ϕ_c	31°
Hardness of granulates, h_s	2.6 GPa
Exponent n	0.27
Minimum void ratio at zero pressure, e_{d0}	0.61
Maximum void ratio at zero pressure, e_{c0}	1.10
Critical void ratio at zero pressure, e_{i0}	0.98
Exponent α	0.14
Exponent β	6
Parameter controlling initial shear modulus upon 180° strain path reversal, m_R	11
Parameter controlling initial shear modulus upon 90° strain path reversal, m_T	6
Size of elastic range, R	2×10^{-5}
Parameter controlling degradation rate of stiffness with strain β_r	0.1
Parameter controlling degradation rate of stiffness with strain χ	1.0

surrounding soil. Because relative pile soil movement and separation between raft and soil can occur during excavations. To incorporate the interactions between pile-soil and raft-soil, surface-to-surface contact technique provided in Abaqus software package (Hibbitt *et al*. 2010) was used. The interface was modelled by the Coulomb friction law, in which the interface friction coefficient (μ) and limiting displacement (γ_{lim}) are required as input parameters. A limiting shear displacement of 5 mm was assumed to achieve full mobilization of the interface friction equal to $\mu\times$p', where p' is the normal effective stress between two contact surfaces, and a typical value 0.35 of μ for a bored pile was used in all analyses (Shi *et al*. 2019). Roller and pin supports were applied to the vertical sides and the base of the mesh, respectively. Therefore, movements normal to the vertical boundaries and in all directions of the base were restrained. The excavation process will be simulated by deactivating soil elements inside twin excavation zones. In the meantime, the truss elements representing the props will be activated.

2.6 Numerical simulation

The numerical simulations of all the three cases were carried out in the following steps

a) Step 1: Initial geostatic stresses were generated in the mesh by applying gravity load and the coefficient of lateral earth pressure of 0.5.
b) Step 2: The piles were constructed then raft was placed on top of pile group and soil deposit.
c) Step 3: The 20-storey building was constructed on top of the piled raft. A live load of 5 kPa was applied on the floor slab of each storey.
d) Step 4: Activate the brick elements representing the diaphragm wall to support the first excavation.
e) Step 5: Staged multi-propped excavation is simulated as described in section 2.1. After excavating to 3 m depth, the first level of props is installed at 1 m below the ground surface.
f) Step 6: Repeat step 6 to excavate the next stages and install props until the last stage of excavation (i.e., He=24 m) is completed.
g) Step 7: Repeating the same procedure as in (Step 5) and (Step 6), the second excavation was carried out.

3. Settlement mechanism of the piled raft during advancement of twin tunnels

3.1 Induced piled raft settlement due to twin excavations

Fig. 4 shows the normalised incremental settlement of the piled raft (S_p/d_p) at due to construction of twin excavations. The excavation stages of each excavation depth are represented by h. The piled raft settlement and excavation depths (h) are normalised by pile diameter (d_p) and final excavation depth (H_e =24 m), respectively. The piled settlement is normalised by the pile diameter. Excavation depths are indicated by h which is normalised by final excavation depth (H_e). It can be seen from the figure that non-linear characteristics of the piled raft were observed with increasing of excavation depth of the first excavation. The rate of S_p increased with each excavation stage. The rate of S_p increased abruptly at excavation stage reaches at h/H_e=0.63 till final excavation depth (h/H_e=1.00).

This was because of degradation of sand stiffness due to excavation-induced stress and the plastic strain generated surrounding the piles due to excavation-induced stress release. Since the initial excavation stages ($0< h/H_e<0.63$) are adjacent to pile shaft, the shafts of the piles were affected by excavation-induced plastic strain. However, the toes of the piles were resting on the intact (from plastic strain) stiffer layer. Whereas, toes of the piles were severely influenced by the plastic strain as excavation stages reaches at the end of excavation. This is because of load transferred borne by the shaft to the pile toes (discussed in section 3.3).

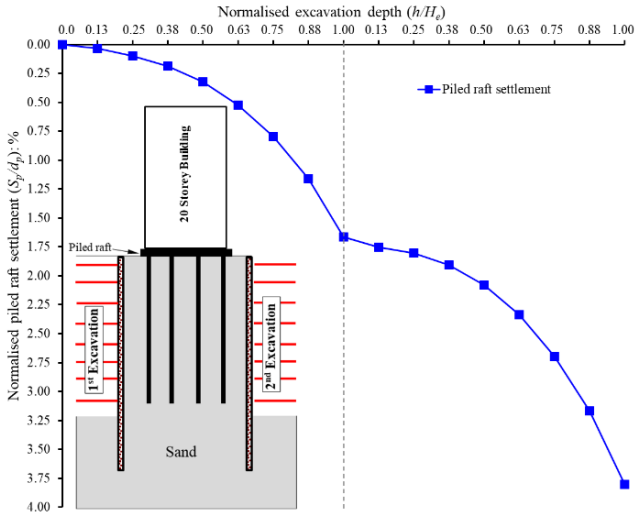

Fig. 4 Induced piled raft settlement during twin excavations

Qualitatively, the second excavation-induced settlement trend with respect to excavation depths is similar to the first excavation-induced settlement. However, the magnitude of the piled raft settlement induced by the second tunnel is higher than that induced by the first excavation. This finding can be ascribed to the variation of the sand stiffness around the piled due to stress release and the development of shear strains as a result of the first excavation.

With settlement due to working load (i.e., 1.48dp%), the total settlements of the building 37 mm (5.3d_p%) is very close to the maximum allowable foundation settlement (i.e., 50 mm) according to Skempton and Macdonald (1956) and O'Brien (2012) Hence, the numerical prediction implies that the serviceability limit state of a building founded on pile can be affected when excavation is carried out adjacent to the building.

3.2 Induced tilting of the building during twin excavations

It is well-recognised that piled raft can reduce differential settlement considerable economy without compromising the safety and performance of the foundation (Poulos 2001). On the other hand, excavation essentially induces stress relief in the ground which resulted in a ground movement towards the excavation. When twin excavations (which are located to the either side of the building) are carried out adjacent to the building, differential settlement can likely be induced in the piled raft. Hence, it is necessary to understand the tilting mechanism of the piled raft during twin excavations. The differential settlement is presented in terms of tilting which is defined as the ratio of the differences in the settlement between the two edges of the piled raft and the distance between the edges. Tilting toward the first excavation is taken as positive vice-versa. Fig. 5(a) illustrates the rate of the induced tilting of the piled raft with excavation stages (h) of twin excavations. It can be observed from the figure that the positive tilting increased non-linearly during the first excavation. The rate of the tilting increases as the excavation depth increases. This is because the piled raft is subjected to the non-uniform and only at one side stress release during the first excavation. The row of piles nearest the first excavation (i.e., front row) is subjected to higher stress release than that of farthest the excavation (i.e., rear row). Consequently, the front row piles settled larger than that of the rear row due to the first excavation which caused differential settlement in the piles. The working load (dead load of the building and live load on the building) was re-distributed among four piles and the raft due to excavation-induced tilting of the piled raft (discussed in section 4.1).

During the subsequent excavation (which is carried out on the other side of the building, see inset in the figure), the measured tilting decreases non-linearly as the depth of the second excavation increases.

As a result, the building tilts towards the second excavation. In contrast to the tilting after the first excavation, the final tilting of the building due to the second excavation (with same depth and system as that of the first excavation) is less than that due to the first excavation. As a result, the building remains tilted towards the first excavation. This excavation-induced settlement mechanism can be attributed to the degradation of sand stiffness around the piled raft due to stress release and the development of shear strains as a result of the first excavation. The stiffness of the soil element surrounding the piled raft degraded due to the first excavation-induced stress release before the second excavation. This ‘‘plastic’’ response implies that the plastic strains generated adjacent to the two excavations overlapped with each other. During the entire process of twin excavations, the most significant transverse tilting occurs at the end of the first excavation. The tilting of the building was computed as 0.85% on completion of the first excavation. Whereas after completion of the twin excavations, the final tilting of the building remained 0.28% which suggest that building is tilted towards the first excavation.

To further illustrate the differential settlement of the building due to adjacent twin excavations, settlements of piled raft induced at various positions along the centreline

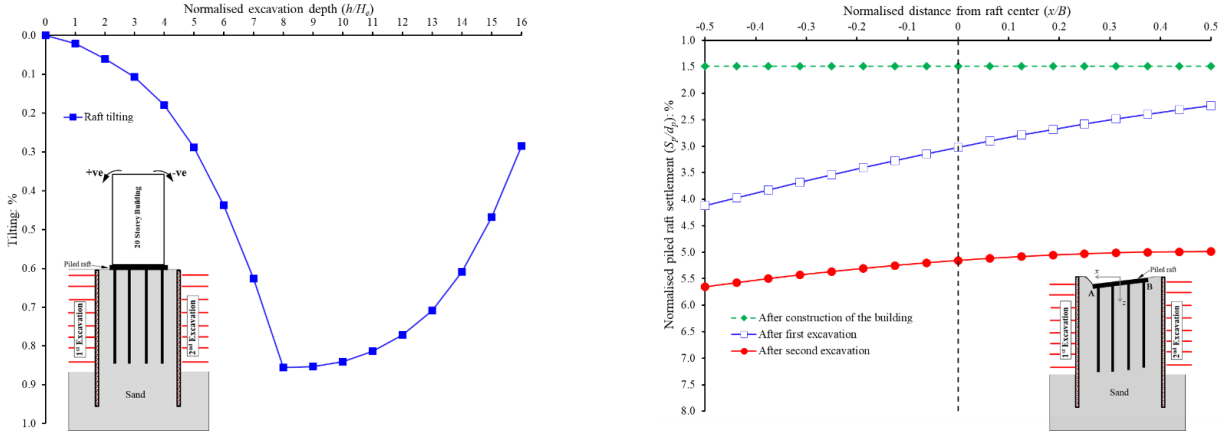

(a) (b)

Fig. 5 (a) Induced tilting of the building during twin excavations and (b) piled raft settlement along the centerline

of the raft (see inset in the figure) due to twin excavations were plotted in Fig. 5(b). In addition, the raft settlement before excavation (i.e., after completion of the building and application of live load on the building) is also included in the figure for reference. It can be seen that after completion of the building construction (before excavation), the settlement occurred in the building was uniform through the centreline of the raft as expected. However, the corner closest to the first excavation (i.e., point A) settled larger than that of farthest (i.e., point B) on completion of the first excavation. The induced differential settlement caused the building permanent inter-storey drifts (discussed in section 3.3). This observation is attributed to excavation-induced stress release which is larger and smaller around pile closest to and farthest from the excavation.

On completion of the second excavation, the corner closets to the second excavation (i.e., point B) settled larger than the farthest (i.e., point A). This is because the piles nearest to the second excavation were subjected to the larger stress release. After careful inspection of the twin excavation induced raft settlement, hogging deformation is induced in the raft due to twin excavation. This observation may be ascribed to the settlement of the piles. The piles located in the mid of the piled raft settled less than that near to the second excavation. Consequently, the raft bend in a hogging profile inducing additional bending moment in the raft (discussed in section 3.4). To avoid any collapse/damage in the buildings, there are guidelines provided by the design codes. Eurocode 7 (CEN, 2001) recommends a wide range of the maximum acceptable tilting (1/2000 to 1/300) for different types of structures (i.e., load-bearing or continuous brick walls, open-framed structures, in-filled frames). Zhang and Ng (2005) provided recommendations of serviceably limit states (i.e., limiting values of building settlement and tilting) based on 57 cases of the buildings resting on deep foundations. They proposed an allowable tilting value of (0.20%) established reliability-based study. Based on the configuration of the geometry, ground conditions, and excavation depths, the induced tilting exceeds the limit values recommended by Zhang and Ng (2005) and Eurocode 7 (CEN, 2001).

3.3 Induced lateral displacement and inter-storey drifts

It is well-recognised that the excavation is essentially a stress-release process. The excavation-induced ground movement towards the excavation led the adjacent building to move laterally. Fig. 6(a) illustrates the lateral movement of each floor of the building during twin excavations. Three different excavation stages (i.e., h/H_e= 0.3, 0.5 and 1.0) of each excavation were selected. It can be seen that the lateral movement of each higher floor is larger than that of its bottom floor. This is because of induced tilting of the pile raft (see Fig. 5(a)).

The lateral movement of each floor along the height of the building increases with depth of the first excavation. This observation is consistent with induced settlement in piled raft. The maximum lateral deflection occurred at the top of the building (the roof level of 20th storey). The general trend of the lateral deflection profile is consistent with differential settlement. On completion of the first excavation, the maximum lateral movement of 60 mm in the 20th floor of the building was computed.

As in to the first excavation, excavation of the second tunnel on the other side of the building resulted in lateral movement of the building towards the second excavation. However, the amount of the lateral movement is smaller than that due to the respective excavation stages of the first excavation. This observation can be attributed to the soil behaviour which highly non-linear and plastic. The significant plastic strains were generated in the ground due to the first excavation which resulted in the lateral movement of the building towards the first excavation. Therefore, the building did not return to its original position due to the second excavation. On completion of the second excavation, the building remained tilted towards the first excavation. Hence, the geotechnical engineers should take this observation into consideration while design the twin excavations adjacent to the building. The final maximum lateral movement of 22 mm at the top floor was computed building.

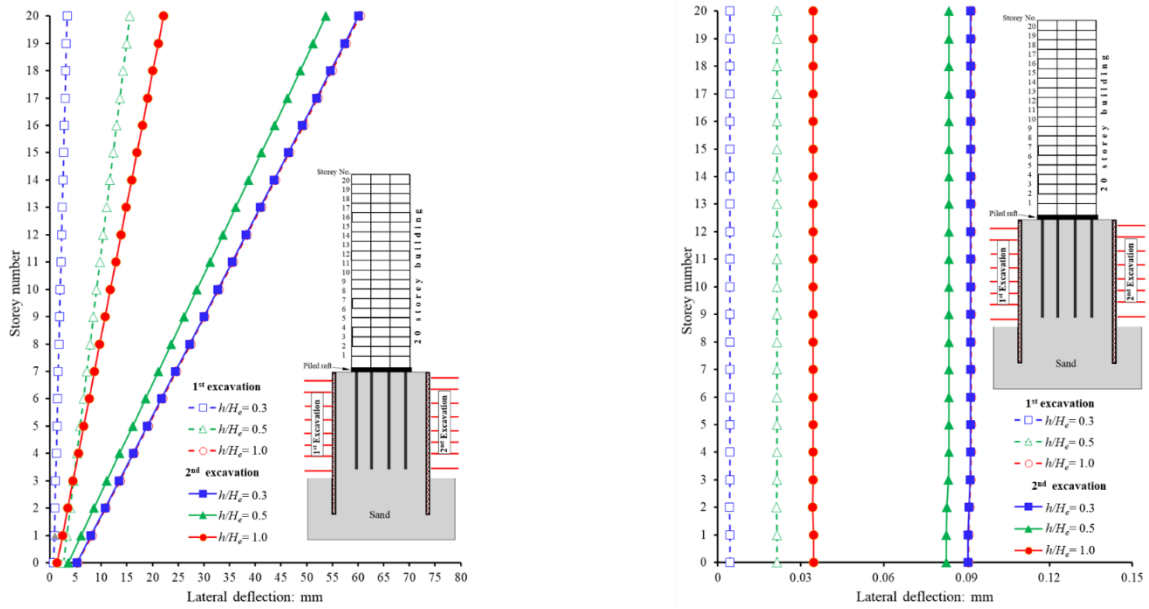

(a) (b)

Fig. 6 (a) Lateral deflection of the building and (b) Inter-storey drift

The lateral movement of the building due to twin excavations caused inter-storey drift which may induce distress in structural component of the building. The inter-storey drift of the building can be defined as ratio of difference of deflections at two storeys to storey height. Fig. 6(b) illustrates inter-storey drift of the building at different depths of twin excavations. It is noted that inter-storey drift shows similar trend as that of lateral deflection due to twin excavations. The maximum value of the drift was computed as 0.09% on completion of the second excavation. The subsequent excavation on the other side of the building resulted in decrease of the building drift which was induced due to the first excavation. This is because the stress relief due to the second excavation was on the other side of the building. Consequently, the ground moves towards the second excavation which led the building drift back. However, the building was not drifted back towards the second excavation because of the plastic behaviour and stiffness degradation of sand. On completion of twin excavations, the final drift magnitude of 0.035% was computed.

The induced tilting and the lateral deflection of the building due to twin excavation can generate substantial plastic strains which can caused cracks in the building. As discussed in section 2.4, the nonlinear concrete behaviour (elasto-plastic) is simulated with a concrete damage plasticity model; in that model, compressive and tensile damage indices (DAMAGEC and DAMAGET, respectively) range between 0 (no damage) and 1 (entire damage).

Figs. 7(a) and 7(b) display the contours of the shear plastic strain and tensile damage index, respectively. It can be seen from the figures that significant plastic strains were generated at the bottom of two middle columns.

Consequently, the most severe tensile cracking damage occurred at the same locations of the building. This implies that the middle two columns of the building underwent significant tension due to excavation-induced tilting and lateral movement. These computed results of generation of plastic strains and tensile damage index due to twin excavations have revealed that care must be taken while planning twin excavations adjacent to any building.

3.4 Induced bending moment in the piled-raft

As discussed in pervious sections, significant differential settlement and lateral movement (hence inter-storey drifts) were induced in the high-rise building due to twin excavations-induced ground movement. The tilting of the building can induce an additional bending moment in the piled-raft due to twin excavations. Since three-dimensional numerical simulation was carried out to investigate the effects on the building, the induced bending moment about both directions (i.e., X and Y axes) were extracted along the centre line of the raft in both directions. Fig. 8(a) shows the induced bending moment in the raft along centre line in X direction (section A-A which is perpendicular to the twin excavations, see inset in the figure) about X and Y axes on completion of the first and the second excavations. It can be observed that the sagging bending moment (with maximum value of 112 kNm at x/B=0.31) was induced in the portion (i.e., x/B<-0.31) of the raft near to the first excavation on completion of the first excavation.

On the other hand, the rest of the portion of the raft (-0.2≤x/B≤0.5) was subjected to the hogging bending moment about X-axis. Similarly, the second excavation caused the sagging moment in the portion of the raft

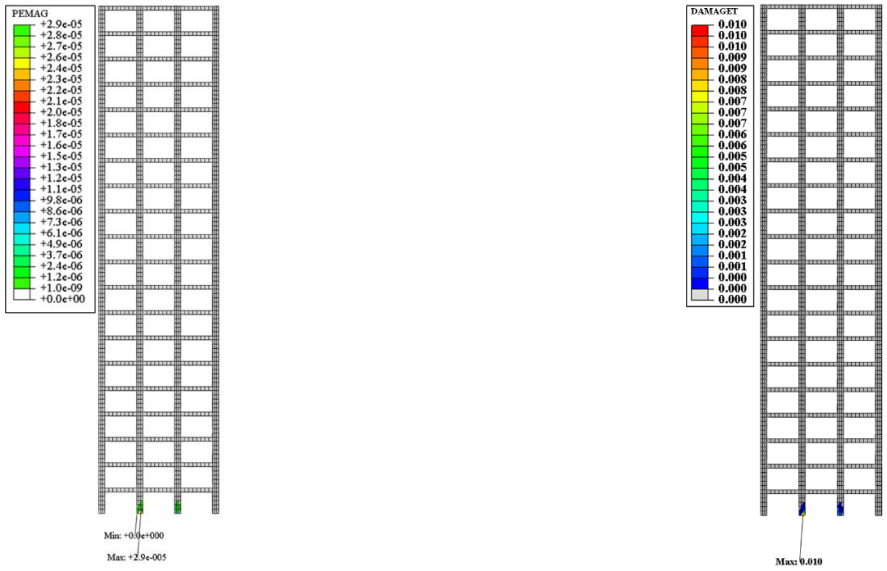

(a) (b)

Fig. 7 Development of (a) plastic stain and (b) tensile crack in the frame after twin excavation

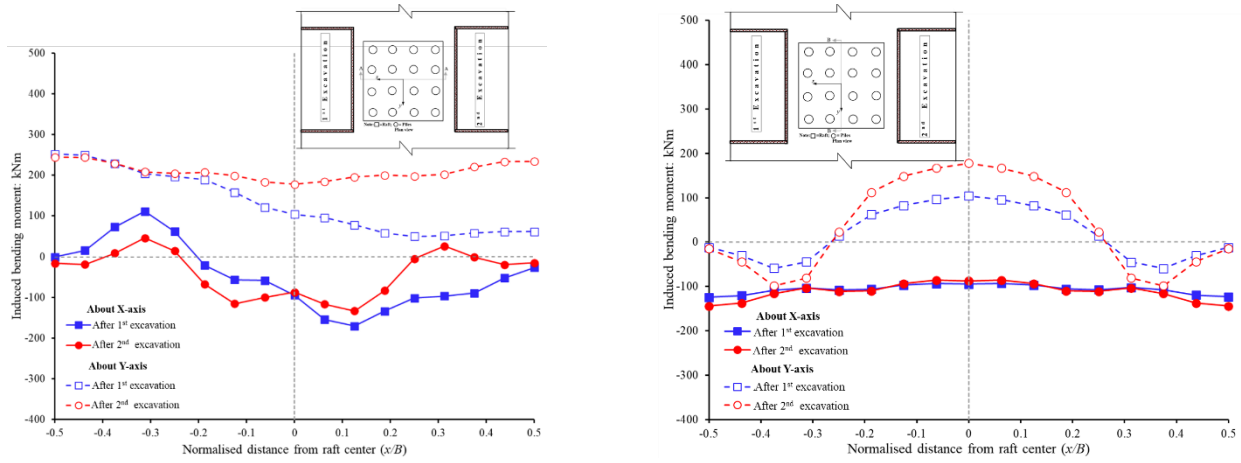

(a) (b)

Fig. 8 Induced bending moment in the raft along centerline (a) X direction and (b) Y direction

(x/B>0.25) near to the second excavation. Whereas, the sagging bending moment (with maximum value of 250 kNm at x/B=-0.5) about Y axis was induced due to the first excavation. However, the induced bending moment decreased along the length of the raft (away from the first excavation). This is because of positive tilting in transverse direction (see Fig. 5) due to the ground movement due to the first excavation (discussed in section 3.5). The soil movement towards the first excavation causing the raft tilted. Consequently, the bending moment about Y axis was induced in the raft. As location of the second excavation is on the other side of the building, the subsequent excavation caused the bending moment about Y axis at end of the raft near the second excavation at x/B=-0.5 (with maximum value of 240 kNm). This is also can be attributed to the soil movement towards the second excavation. Compared to the induced bending moment about X-axis along section A-A, the bending moment along Y axis is larger. This is because of the significant tilting in transverse direction.

3.5 Induced soil movement and shear strain due to the first and the second excavations

To further understand the settlement mechanism of the building due to twin excavations, the ground movement vectors and shear stain contours of selected section (i.e., along the centreline and perpendicular to twin excavations) were drawn.

Fig. 9(a) shows computed incremental displacement vectors due to the first excavation. In addition, computed incremental shear strain the excavation induced stress release is also superimposed in the figure. It can be observed that soil on the retained side moved towards the excavation, whereas the soil underneath the excavation heaved upwards due to vertical stress relief inside the exaction zone.

Furthermore, it can be seen that soil movement near the first excavation is larger than that of away from the diaphragm wall. Moreover, the ground movement generate

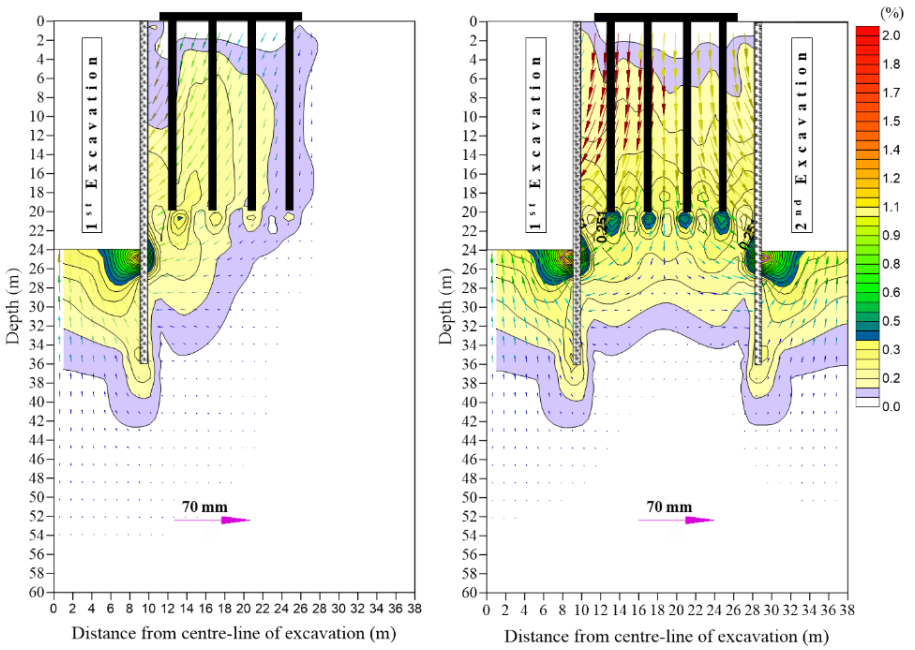

Fig. 9 Induced displacement vectors and shear strain contours after (a) the first excavation and (b) twin excavations

the substantial shear strain around the excavation. This can be attributed to the stress release during excavation. The subsurface ground movement due to the first excavation appears at the ground surface in the shape of Gaussian curve. The ground surface settlement near the excavation is maximum and decrease exponentially away from the excavations. The ground surface movement caused the high-rise building resting on the piled raft tilted (see Fig. 5) and moved laterally (see Fig. 6(a)) towards the first excavation. Consequently, the lateral movement (hence inter-storey drift) and bending moment was induced in the building and the raft, respectively. The significant ground movement and shear strain also altered the load transfer among the raft and piles (discussed in section 4.1).

After the completion of second excavation which is located on the other side of the building, the direction of the vectors of the soil movement was towards the second excavation. The displacement vectors at middle portion of the piled raft after twin excavations revealed that the soil movement is in vertical direction. This is because the direction of displacement vectors of the soil movement at the raft middle due to the first excavation is towards the first excavation. The net movement after twin excavation becomes downward. The ground movement due to excavation-induced stress release generated significant shear strains. The shear strains contours suggested that the piled raft is within the substantial shear strains zone. As a result, the high-rise building settled (see Fig. 4) and moved laterally (see Fig. 6(a)) and tilted towards the second excavation decreasing the titling which was induced due to the first excavation (see Fig. 5). However, the building did not return to its original position because of degradation of the sand due to shear stain in the ground. Moreover, the second excavation further caused the load re-distribution in the piled raft (discussed in section 4.1).

4. Load transfer mechanism of the piled raft during advancement of twin tunnels

4.1 Changes in load sharing between raft and piles

After construction of the building resting on a piled raft system, some of the building load is sustained by the raft and remaining load is transferred to the piles. However, the load taken by the raft can be altered when twin excavations were carried out adjacent to the high-rise building. Fig. 10 shows the change in load sharing by the raft during different construction stages of twin excavation. It can be seen that before excavation (after application of working load), about 32% of the building load (i.e., 65.8 MN) was carried by the raft and rest of the load was transferred to sixteen piles. It can be observed that the load taken by the raft kept decreasing during the first excavation. The rate of reduction of the load decrease when the first excavation reaches at h/He=0.75. This is because of ground surface settlement (see Fig. 9) is larger than that of piled raft (see Fig. 4). The raft separated from the ground surface and resulted in the load (which was taken by the raft) transferred to the piles. This caused reduction in the vertical stress in the ground after completion of the first excavation (discussed in section 4.2). On completion of the excavation the load resisted by the raft reduced to 21.1% of the total load. Similarly, the load taken by the raft further decreased during the second excavation. However, the rate of reduction of the load due to the second excavation is smaller than that due to the first excavation. This is because the induced raft settlement due to the second excavation is larger than that due to the second excavation (see Fig. 4). As a result, the raft remains in contact with the ground. Consequently, the load transfer from the raft to the piles due to the second excavation is smaller than that due to the first excavation. This caused further reduction in vertical stress in the ground (discussed in section 4.2). On

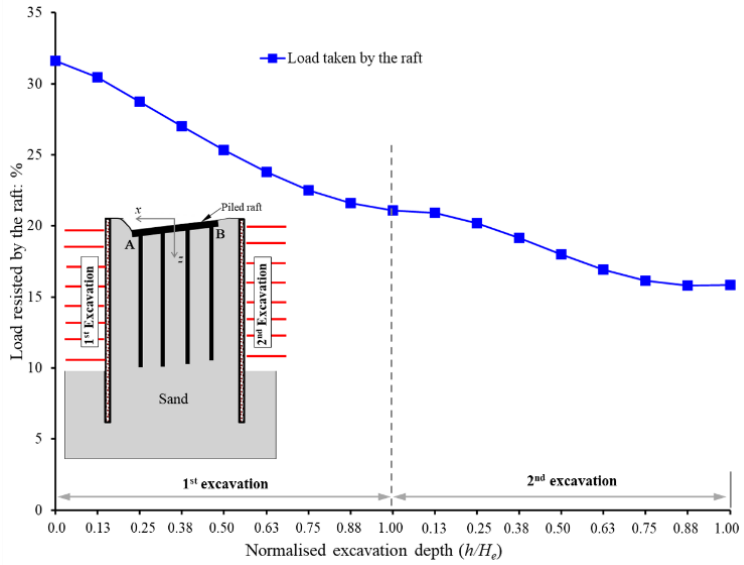

Fig. 10 Changes in load resisted by the raft during excavation

completion of twin excavations, the load taken by the raft was 16% of the total load. These results show that additional loads on the piles should be taken in account when planning twin excavations adjacent to the buildings in a practical scenario.

4.2 Changes in vertical stresses underneath the raft and stress path evolution

As discussed earlier, the significant changes were induced in load sharing by the raft during the twin excavation. These changes resulted in substantial changes in vertical stresses in the ground. For this, soil elements along the centreline (section A-A, see inset in Fig. 11(a)) are selected to investigate contact pressure (Q) underneath the raft. Fig. 11(a) shows the contact pressure underneath the raft on completion of the first and second excavations. The horizontal distance from the raft centre was normalized by the raft width (B). For reference, the contact pressure after completion of the building and application of live load (i.e., before twin excavations) are included. As expected, uniform distribution of Q was generated underneath the raft prior to twin excavations. Owing to stress release due to the first excavation, the contact pressure decreases substantially along the entire centreline of the raft on completion of the first excavation. The region closets to the first excavation underwent larger reduction of the stresses (reduction of 64 kPa at x/B=-0.4). This reduction in stresses caused the load which was resisted by the raft transferred to the piles (see Fig. 10). This can be attributed to excavation induced soil movements and stress release beneath the raft. Ng *et al.* (2021) reported the formation of the gap between a (2×2) raft and the ground due to excavation in dry sand. As a result, the contact pressure became zero in the ground in their study. But the residual net contact pressure after the first excavation implies that no any gap was developed between the raft and the ground in this study. It implies that the formation of the gap between the raft and the ground highly depends upon the ground condition, excavation depth and number of piles in the piled raft. Similarly, the contact pressure further decreased on completion of twin excavations. The portion of the raft near second excavation was subjected to larger stress reduction after completion of twin excavations. This is because the induced ground movement due to twin excavations is larger than that of piled raft. As a result, the load taken by the raft further transferred to the piles (discussed in section 4.3). On completion of twin excavations, residual contact pressures of 10 kPa, 30 kPa and 4 kPa was computed at x/B=-0.5, 0 and +0.5, respectively.

To further illustrate the load transfer mechanism from raft to the piles, stress path evolution of a soil element (located underneath and centre of the raft, see inset in Fig. 11(b)) is investigated. Fig. 11(b) computed stress paths of selected soil element. The K_0 (at-rest earth pressure coefficient) line and critical state line are also shown in the figure for reference. It can be seen that the initial stress states of the selected soil element in both cases are at K_0 stress condition as expected. After completion of construction of building and application of live load on the building slabs, the mean effective stress (p') and deviatoric stress (q) of the selected soil element increased (moving towards critical state line). Owing to stress release and ground movement due to the first excavation, p' and q decreased moving back to K_0 line. The rate of reduction of both p' and q increased as the excavation stages of the first excavation (E1 to E8) increased. This observation suggests that load resulted by the raft transferred to the piles (see Fig. 10). On completion of the first excavation, the stress path of the selected element moves to K_0 line. During subsequent excavation, there was further decrease in p' and q, caused by ground movement due to the excavation induced stress release (see Fig. 9(b)). This can be attributed to the load transfer from the raft to the piles. On completion of twin excavations, the stress state of the soil element under the raft stayed slightly below the K_0 line.

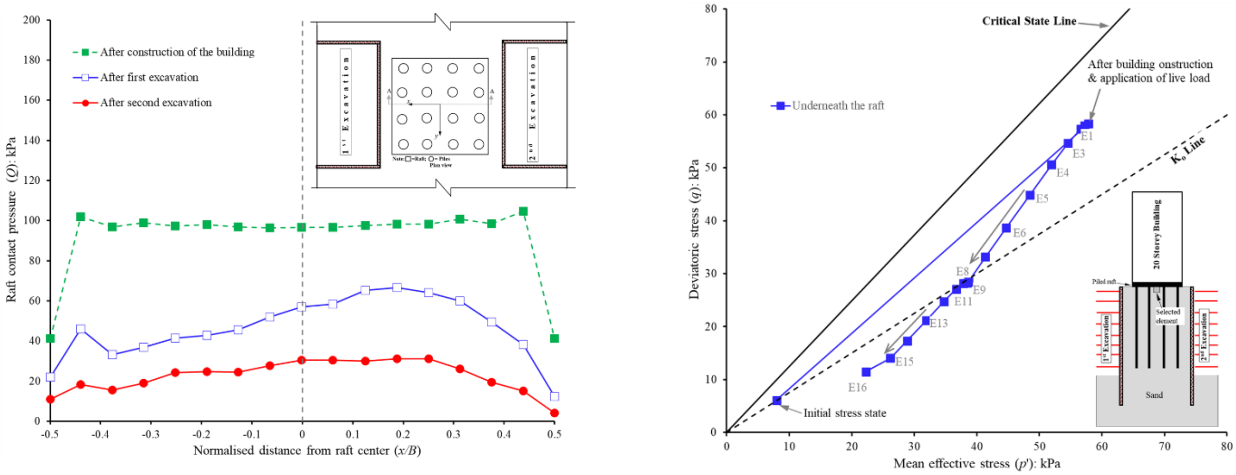

(a) (b)

Fig. 11 Changes in vertical stresses along centerline of the raft (b) Evolution of stress path of a selected element underneath the raft

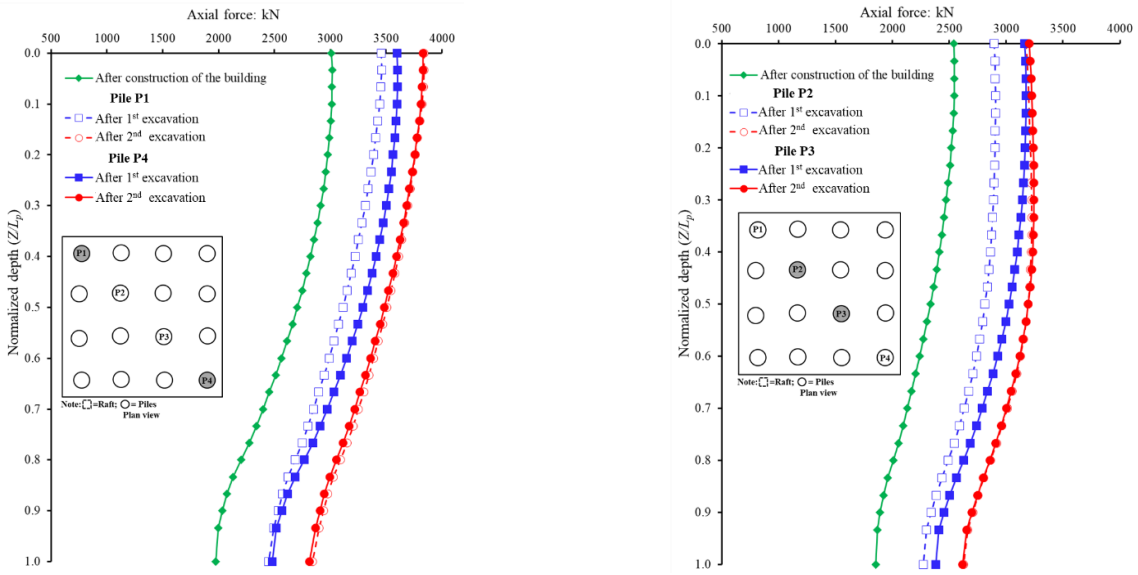

(a) (b)

Fig. 12 Changes in axial load (a) piles P1& P4 and (b) piles P2 and P3

4.3 Changes in axial load distribution along piles due to twin excavations

As discussed in previous section, the load resisted by the raft decreased on completion of twin excavations. Hence the load transfer to the piles in the piled raft system which is in square pattern (i.e., 4×4 piles). Among 16 piles, the piles at critical positions are selected for discussion in this section. The piles are designated as P1, P2, P3 and P4 (see the inset in Fig. 12). Fig. 12(a) compares axial load distribution along the lengths of piles P1 and P4 which are positioned at the corner of the raft. For comparison, load distribution along the length of each pile before the excavation is included in each figure. Prior to twin excavations, same amount of load (i.e., 2540 kN) is taken by the pile P1 and P4. Therefore, the load distribution along the both piles are identical. The shaft resistance and end-bearing of both piles contributed to the resist the 34% and 66% of the load transferred to the piles, respectively. The load along the entire pile lengths of both the piles increased on completion of the first excavations. This is because the load taken by the raft transferred to the piles (see Fig. 10) resulted in increment in head loads of the piles. The load taken by pile P4 is larger than that by pile P1. This is because locations of pile P1 and pile P4 is nearest and farthest from the first excavation. Therefore, the pile P1 is subjected to higher stress release than that of pile P4. This indicates that shaft resistance decreased along the length of

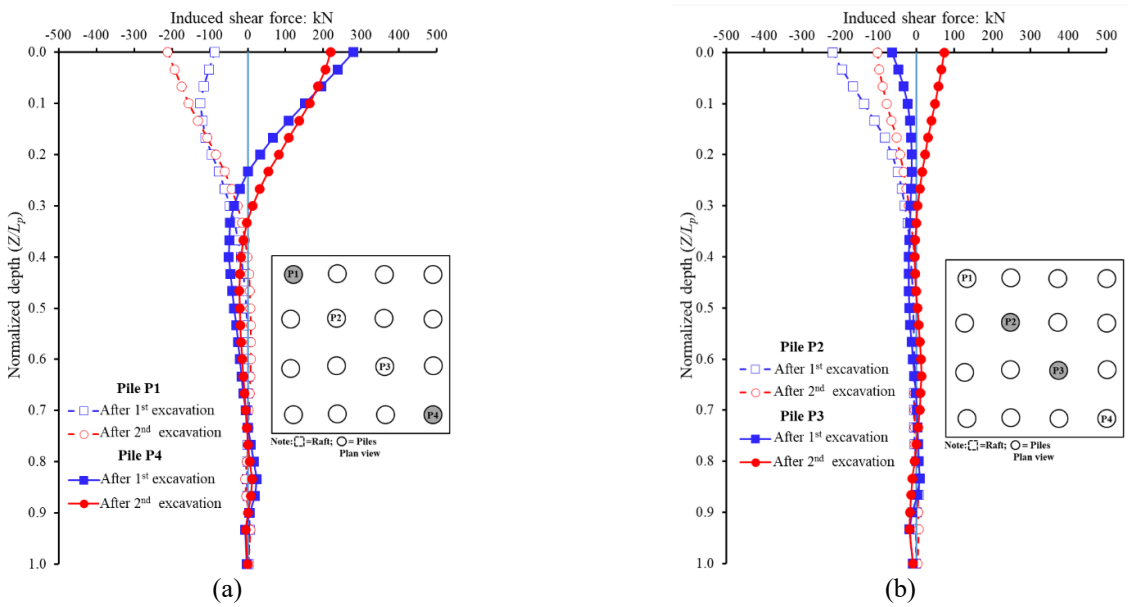

Fig. 13 Induced shear force along length of (a) piles P1& P4 and (b) piles P2 and P3

both the piles. This observation can be attributed to excavation-induced shear stain due to stress release at the mid-portion of the pile. The shaft resistance along the upper part of the piles was transferred downward to the pile toes, leading to a 24% and 26% increase in mobilised end-bearing resistance of piles P1 and P4, respectively. On completion of the second excavation (which is located on the other side of the building), the load along the entire length of piles further increased because of the load transferred from the raft. Owing to stress release due to excavations, the load borne by the pile shafts transferred to the toe of piles. Consequently, the mobilised end-bearings of both piles increased to 44%.

Fig. 12(b) compares axial load distribution along the lengths of piles P2 and P3. For comparison, load distribution along the length of each pile before the excavation is included in each figure.

It can be seen from the figure that before excavation the load transferred to each of pile P2 and P3 was 2540 kN. The piles resisted the load by mobilising shaft resistance (27% of load) along lower portion the pile lengths and remainder 73% of the load was resisted by end-bearing. It can be seen from the figure that similar to the changes in axial load distribution along pile lengths of P1 and P4, the axial load along the entire pile lengths of P2 and P4 increased on completion of the excavation. This load redistribution is ascribed to excavation-induced stress release and load transfer from the raft to piles. The end-bearing of both the piles P2 and P3 increased by 30% to carry the transferred load from the raft. Similarly, the load along the entire length of piles P2 and P4 further increased because of the load transferred from the raft on completion of the second excavation (which is located on the other side of the building). Owing to stress release due to excavations, the load borne by the pile shafts transferred to the toe of piles.

Consequently, the mobilised end-bearings of both piles increased to 42%.

4.4 Induced shear forces along piles due to twin excavations

Prior to excavations, the piles are horizontally confined by the surrounding soil and are subjected to negligible shear forces and bending moments. However, excavation induces stress release and ground movement around the piles causing shear forces and bending moment in the piles. Fig. 13 illustrates the induced shear forces along normalised depth of piles P1 and P4 on completion of the first and the second excavations. As a sign convention, positive value of shear force indicated the direction towards the first excavation and vice versa. The profiles of induced shear force along the length of piles were highly non-linear. It can be observed that negative shear force was induced at the upper portion of the pile P1 ($Z/L_p \leq 0.25$) due to the first excavation. However, negligible shear forces were induced in the lower portion of the piles. This is because of the soil displacement towards the first excavation-induced stress release and shear strain (see Fig. 9). Owing to excavation-induced intensive shear strain zone generated, the pile raft tilted towards the first excavation (see Fig. 5(a)). The lateral forces on the piles are hence a reaction to a forced movement of the piled raft. The maximum lateral force of 86 kN (away from the first excavation) was induced at the pile head. After subsequent excavation the lateral force further increased to 212 kN. This is because piled raft tilted back as result of that the second excavation induced-shear strain generated around the piled raft (see Fig. 9). The tilting of the pile raft on the opposite side has increased the reaction (i.e., lateral forces on the pile).

Unlike the induced shear force in pile P1 due to twin excavation, positive shear forces were induced at the upper portion of pile P4. This is because all the piles are rigidly connected to the raft. The raft pulling pile P4 towards the first excavation causing the positive shear force. The maximum shear force of 280 kN was induced at the pile

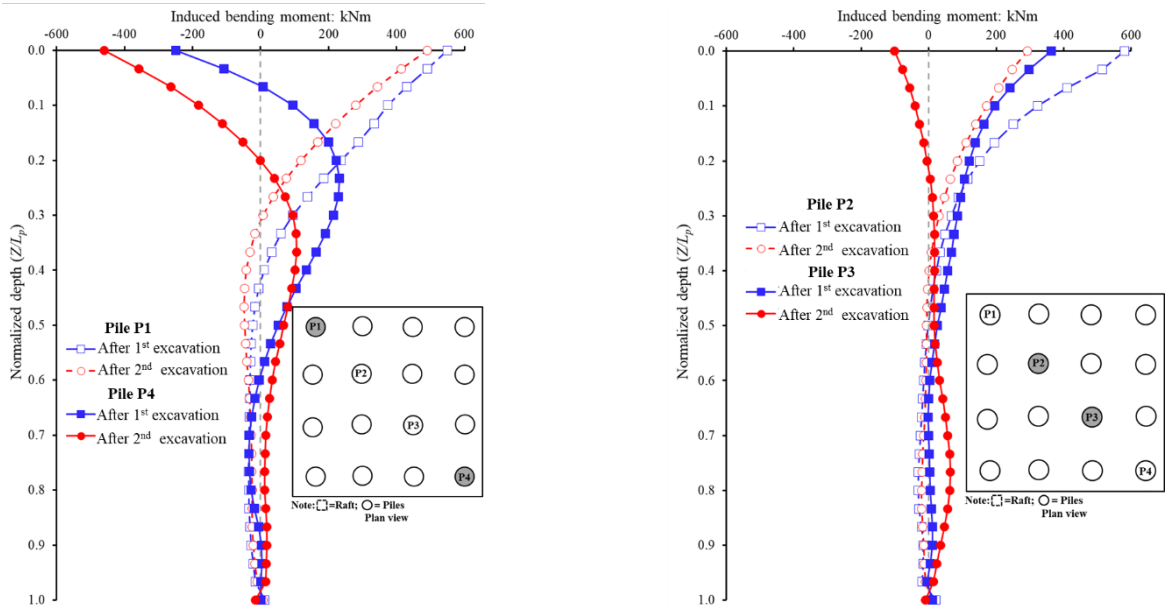

(a) (b)

Fig. 14 Induced bending moment along length of (a) piles P1& P4 and (b) piles P2 and P3

head. On completion of the second excavation, the induced shear forces along pile P4 decreased slightly. This because the second excavation is located on the other side of the building. The final value of shear force 220 kN towards the first excavation was computed at the head of pile P4. Similar induced shear forces profile along pile P2 and pile P3 were induced in completion of the first and second excavations, as illustrated in Fig. 13(b). However, the magnitude of the forces is smaller than that induced in piles P1 and P4. This is because of location of both piles in the piled raft system. Both piles are located in the mid of the raft. Therefore, these are subjected to push and pull on either side of the piles from the raft due to twin excavations. The maximum shear forces of 50 kN and 75 kN were developed at the pile head of piles P2 and P3, respectively.

4.5 Induced bending moments along piles due to twin excavations

The ground movement due to excavation-induced stress release can induced bending moment in the foundation (i.e., piled raft) of the building. Since the piles are not usually designed to sustain bending moment, the bending moment induced in the piles is another important parameter to investigate due to adjacent excavation (Jamil and Ahmad, 2018). Fig. 14(a) shows the induced bending moments along normalised depth of piles P1 and P4 on completions of the first and second excavations.

A positive bending moment means that tensile stress was induced along the pile shaft facing the first excavation. It can be seen from the figure that the maximum bending moment induced at head of pile P1 after completion of the first excavation. This is because the piles are rigidly connected to the raft and lateral soil movement due to the first excavation induced stress release and (see Fig. 9). This negative bending moment was counter-balanced by the positive bending moment in the lower portion of the pile (Z/L_p>0.13). The maximum bending moment of 550 kNm was induced at the pile head of P1. Subsequently, the piled raft was subjected to stress release on the other side due to the second excavation, the induced bending moment further decreased along the length of the pile P1. This is because of ground movement towards the second excavation and resulted in net soil movement in vertical direction due to twin excavations (see Fig. 9). Finally, a positive bending moment of 490 kNm was induced at the pile head. Unlike the induced bending moment in pile P1 due to twin excavation, negative bending moment induced the upper part of pile P4 (Z/L_p>0.03). This is because all the piles are rigidly connected to the raft. The raft pulling pile P4 towards the first excavation causing the negative bending moment. To counter-balance the negative bending moment, positive bending moment was induced at lower portion of the pile. The maximum bending moment of 250 kNm was induced at the pile head of P4. On completion of the second excavation, the induced bending moment along pile P4 increased at the upper part of pile P4. This is because the second excavation is located on the other side of the building. The final value of shear force 460 kNm was computed at the head of pile P4. Similar bending moment profile along pile P2 and pile P3 were induced on completion of the first and second excavations, as illustrated in Fig. 14(b). However, the magnitude of the bending moment is smaller than that induced in piles P1 and P4. This is because of location of both piles in the piled raft system. Both piles are located in the mid of the raft. Therefore, these are subjected to push and pull on either side of the piles from the raft due to twin excavations. On completion of twin excavations, the maximum bending moment of +290 kNm and -101 kNm were developed at the pile head of piles P2 and P3, respectively.

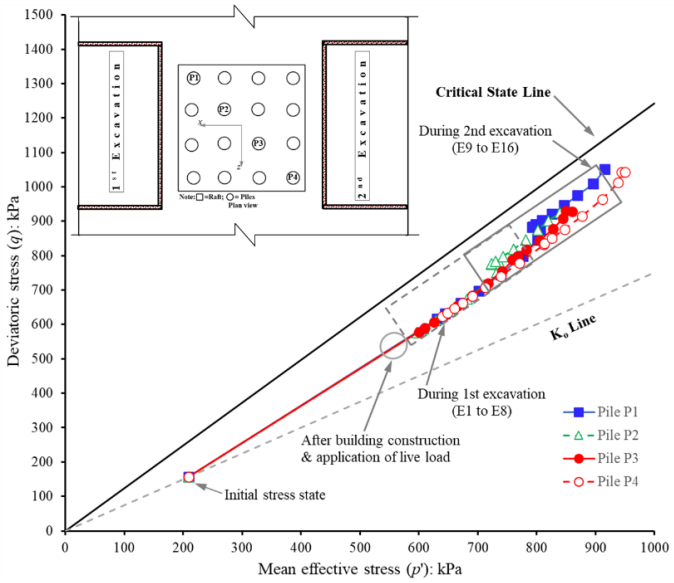

Fig. 15 Evolution of stress path of the selected elements underneath the piles P1, P2, P3 and P4

4.6 Computed stress path evolution underneath the pile toes during twin excavations

Fig. 15 illustrated computed stress paths evolution of a soil elements located right below the piles P1, P2, P and P4 (see inset in the figure) during different excavation stages of the first and second excavations. The K_0 (at- rest earth pressure coefficient) line and critical state line are also shown in the figure for reference.

It can be seen that the initial stress states of the selected soil elements were experiencing K_0 stress condition as expected. After completion of construction of building and application of live loads on floor of the building, both the mean effective stress (p') and deviatoric stress (q) of the selected soil elements increased moving towards the critical state line. As the first excavation (from E1 to E8) proceeds, both p'and q increased due to downward stress transfer from the pile shafts to the pile toes (see Fig. 12). As a result, the stress path moved towards the critical state line and reached failure once the excavation reaches E6 (h/H_e= 0.75). The second excavation (from E9 to E16) resulted in further increases in both p'and q at a lower rate than that during the first excavation. This is because the downward stress transfer during the second excavation was more substantial than that during the first excavation (see Fig. 12). As a result, the stress path moved beyond the critical state line. Consequently, significant shear strain generated underneath the toes of the piles (see Fig. 9).

5. Conclusions

In this study, three-dimensional numerical simulation was carried out to evaluate the performance of a 20-storey frame building subjected to ground movement due to twin excavations (which were carried out on the either side of the building) ground (sand) movement. An advanced hypoplastic sand model (which can capture small-strain stiffness and stress-state dependent dilatancy of sand) was adopted. The concrete damaged plasticity (CDP) model was used to capture the cracking behaviour in the concrete beams, columns and piles. The responses of the building and foundation in terms of permanent inter-story drifts, raft displacement, forces and bending moments in the raft and pile during different stages of twin excavations. Based on sand density, excavation depths and the high-rise building geometry, the following conclusions are drawn:

(a) The first excavation-induced stress release and ground movement induced substantial differential settlement (i.e., tilting) in the adjacent high-rise building which caused cracks in the frame of the building. Whereas, the second excavation caused the building tilt back with smaller rate. As a result, the building remains tilted towards the first excavation with final value of tilting of 0.28% that exceeds the allowable limit (0.2%) suggested by Eurocode 7 (CEN, 2001).

(b) The tilting of the due to twin excavations building induced an additional two-ways bending moments in the raft. Owing to positive final tilting due to the twin excavations, the sagging bending moment about Y axis (with the maximum value of 250 kNm at x/B=-0.5) was induced along the raft width (perpendicular to the excavations). On the other hand, the twin excavations (on either side of the building) caused the hogging bending moment at the middle portion of the raft and sagging bending moment at the end of the raft along the raft width (parallel to the excavations).

(c) The first excavation resulted in displace the high-rise building laterally towards the excavation which caused the building permanent inter-storey drifts. As in to the first excavation, excavation of the second tunnel on the other side of the building resulted in lateral movement of the building towards the second excavation with smaller rate. Therefore, the building did not return to its original position due to the second excavation. The final maximum lateral movement of 22 mm at the top floor was computed building.

(d) The inter-storey drift caused significant plastic strains at the bottom of two middle columns. Consequently, the most severe tensile cracking damage occurred at the same locations of the building. These computed results of generation of plastic strains and tensile damage index due to twin excavations have revealed that care must be taken while planning twin excavations adjacent to any building.

(e) Owing to the stress-release and surface settlement due to twin excavations (which either side of the building), the load taken by the raft (before excavation) reduced significantly. On completion of twin excavations, the load resisted by the raft reduced to half (16% of the total load) of that the load before the excavations (32% of the total load). The reduced load transferred to the piles.

(f) As a result of load transfer from the raft to the piles and stress release due to twin excavations, the axial load along the entire length of piles increased. The load borne by the pile shafts transferred to the toe of piles. Consequently, the mobilised end-bearings of both piles increased significantly.

(g) Due to rigid connection between the raft and piles, significant shear forces and bending moment induced at the upper portion of piles ($Z/L_p \leq 0.25$) with the maximum at the pile head on completion of twin excavations. Hence, it may also be necessary to assess the piles structural rigidity while assessment of excavations adjacent to the building.

It should be noted that the computed results reported in this paper should be treated with caution since they may be specific to the particular conditions modelled.

Acknowledgments

The authors would like to acknowledge the financial support provided by Mehran University of Engineering & Technology, Jamshoro, Sindh and Pakistan.

Conflicts of Interest

The authors declare that they have no conflicts of interest.

References

Atkinson, J.H., Richardson, D. and Stallebrass, S.E.. (1990), "Effect of recent stress history on the stiffness of overconsolidated soil", *Géotechnique*, **40**(4), 531-540. https://doi.org/10.1680/geot.1990.40.4.531.

Boone, S.J., Westland, J. and Nusink, R. (1999), "Comparative evaluation of building responses to an adjacent braced excavation, *Can. Geotech. J.*, **36**(2), 210-223. https://doi.org/10.1139/t98-100.

Ding, Z., Wei, X.J. and Wei, G. (2017), "Prediction methods on tunnel-excavation induced surface settlement around adjacent building", *Geomech. Eng.*, **12**(2), 185-195. https://doi.org/10.12989/gae.2017.12.2.185.

CEN (2001), Eurocode 7, part 1: Geotechnical design: General rules, Final Draft prEN 1997-1. Brussels, Belgium: European Committee for Standardization (CEN).

Finno, R.J., Lawrence, S.A., Allawh, N.F. and Harahap, I.S. (1991), "Analysis of performance of pile groups adjacent to deep excavation", *J. Geotech..Eng.*, **117**(6), 934-955. https://doi.org/10.1061/(ASCE)0733-9410(1991)117:6(934).

Fang, J., Kong, G. and Yang, Q. (2022), "Group performance of energy piles under cyclic and variable thermal loading", *J. Geotech. Geoenviron. Eng.*, **148**(8), 04022060. https://doi.org/10.1061/(ASCE)GT.1943-5606.0002840.

Goh, A.T.C., Wong, K.S., Teh, C.I. and Wen, D. (2003), "Pile response adjacent to braced excavation", *J. Geotech. Geoenviron. Eng.*, **129**(4), 383-386. https://doi.org/10.1061/(ASCE)1090-0241(2003)129:4(383).

Gudehus, G. (1996), "A comprehensive constitutive equation for granular materials", *Soils Found.*, **36**(1), 1-12. https://doi.org/10.3208/sandf.36.1.

Herle, I. and Gudehus, G. (1999), "Determination of parameters of a hypoplastic constitutive model from properties of grain assemblies", *Mech. Cohesive-frictional Mater.*, **4**(5), 461-486. https://doi.org/10.1002/(sici)10991484(199909)4:5%3C461::aid-cfm71%3E3.0.co;2-p.

Hibbitt, D., Karlsson, B.I. and Sorensen, E.P. (2010), Abaqus user's manual, version 6.10.2. Hibbitt, Karlsson & Sorensen Inc;, Providence, RI, USA.

Hong, Y., Ng, C.W.W., Liu, G.B. and Liu, T. (2015), "Three-dimensional deformation behaviour of a multi-propped excavation at a "greenfield" site at Shanghai soft clay", *Tunn. Undergr. Sp. Tech.*, **45**, 249-259. https://doi.org/10.1016/j.tust.2014.09.012.

Hsiao, E.C., Schuster, M., Juang, C.H. and Kung, G.T. (2008), "Reliability analysis and updating of excavation-induced ground settlement for building serviceability assessment", *J. Geotech. Geoenviron. Eng.*, **134**(10), 1448-1458. https://doi.org/10.1061/(ASCE)1090-0241(2008)134:10(1448).

Ishihara, K. (1993), "Liquefaction and flow failure during earthquakes", *Géotechnique*, **43**(3), 351-415. https://doi.org/10.1680/geot.1993.43.3.351.

Jáky, J. (1944), "The coefficient of earth pressure at rest", *J. Soc Hungarian Arch. Eng.*, 355-8 [in Hungarian].

Jamil, I. and Ahmad, I. (2019), "Bending moments in raft of a piled raft system using Winkler analysis", *Geomech. Eng.*, **18**(1), 41-48. https://doi.org/10.12989/gae.2019.18.1.041.

Karira, H., Kumar, A., Ali, T.H., Mangnejo, D.A. and Mangi, N. (2022), "A parametric study of settlement and load transfer mechanism of piled raft due to adjacent excavation using 3D finite element analysis", *Geomech. Eng.*, **30**(2), 169-185. https://doi.org/10.12989/gae.2022.30.2.169.

Korff, M., Mair, R.J. and Van Tol, F.A.F. (2016), "Pile-soil interaction and settlement effects induced by deep excavations", *J. Geotech. Geoenviron. Eng.*, **138**(7), 04016034. https://doi.org/10.1061/(ASCE)GT.1943-5606.0001434.

Liyanapathirana, D.S. and Nishanthan, R. (2016), "Influence of deep excavation induced ground movements on adjacent piles", *Tunn. Undergr. Sp. Tech.*, **52**, 168-181. https://doi.org/10.1016/j.tust.2015.11.019.

Lee, S.W. (2019), "Experimental study on effect of underground excavation distance on the behavior of retaining wall", *Geomech. Eng.*, **17**(5), 413-420. https://doi.org/10.12989/gae.2019.17.5.413.

Long, M. (2001), "Database for retaining wall and ground movements due to deep excavations", *J. Geotech. Geoenviron. Eng.*, **127**(3), 203-224. https://doi.org/10.1061/(ASCE)1090-0241(2001)127:3(203).

Lubliner, J., Oliver, J., Oller, S. and Onate, E. (1989), "A plastic-damage model for concrete", *Int. J. Solids. Struct.*, **25**(3), 299-326. https://doi.org/10.1016/0020-7683(89)90050-4.

Mu, L., Huang, M., Roodi, G.H. and Shi, Z. (2021), "Allowable wall deflection of braced excavation adjacent to pile-supported buildings", *Geomech. Eng*., **26**(2), 161-173. https://doi.org/10.12989/gae.2021.26.2.161.

Maeda, K. and Miura, K. (1999), "Relative density dependency of mechanical properties of sands", *Soils Found.*, **39**(1), 69-79. https://doi.org/10.3208/sandf.39.69.

Niemunis, A. and Herle, I. (1997), "Hypoplastic model for cohesionless soils with elastic strain range", *Mech. Cohesive-frictional Mater*., **2**(4), 279-299. https://doi.org/10.1002/(SICI)1099-1484(199710)2:4<279::AID-CFM29>3.0.CO;2-8

Ng, C.W., Wei, J., Poulos, H. and Liu, H. (2017), "Effects of multipropped excavation on an adjacent floating pile", *J. Geotech. Geoenviron. Eng.*, **143**(7), 04017021. https://doi.org/10.1061/(ASCE)GT.1943-5606.0001696.

Ng, C.W.W., Shakeel, M., Wei, J. and Lin, S. (2021), "Performance of existing piled raft and pile group due to adjacent multipropped excavation: 3D centrifuge and numerical modeling", *J. Geotech. Geoenviron. Eng.*, **147**(4), 04021012.

Poulos, H.G. (2001), "Piled raft foundations: design and applications", *Géotechnique*, **51**(2), 95-113. https://doi.org/10.1680/geot.2001.51.2.95.

O'Brien, A.S. (2012), "Chapter 52 Foundation types and conceptual design principles", *ICE manual of geotechnical engineering*, **2**, 733-764.

Qian, J. Tong, Y. Mu, L. Lu, Q. and Zhao, H. (2020), "A displacement controlled method for evaluating ground settlement induced by excavation in clay", *Geomech. Eng*., **20**(4), 275-285. https://doi.org/10.12989/gae.2020.20.4.275.

Shi, J., Wei, J., Ng, C.W.W. and Lu, H. (2019), "Stress transfer mechanisms and settlement of a floating pile due to adjacent multi-propped deep excavation in dry sand", *Comput. Geotech*., **116**, 103216. https://doi.org/10.1016/j.compgeo.2019.103216.

Shi, J., Chen, Y., Lu, H., Ma, S. and Ng, C.W.W. (2022a), "Centrifuge modeling of the influence of joint stiffness on pipeline response to underneath tunnel excavation", *Can. Geotech. J.*, (Online). https://doi.org/10.1139/cgj-2020-0360.

Shi, J., Wei, J., Ng, C.W., Lu, H., Ma, S., Shi, C. and Li, P. (2022b), "Effects of construction sequence of double basement excavations on an existing floating pile", *Tunn. Undergr. Sp. Tech*., **119**, 104230. https://doi-org/10.1016/j.tust.2021.104230.

Skempton, A.W. and Macdonald, D.H. (1956), "The allowable settlement of building", *Proc. Inst Civil Eng*., **5**(6), 727-768.

Soomro, M.A., Mangi, N., Memon, A.H. and Mangnejo, D.A. (2022), "Responses of high-rise building resting on piled raft to adjacent tunnel at different depths relative to piles", *Geomech. Eng.*, **29**(1), 25-40. https://doi.org/10.12989/gae.2022.29.1.025.

Standards Australia (2002), "Structural design actions; Part 1 Permanent, imposed and other actions", AS1170.1, Sydney Australia: Standards Australia.

Zhang, R., Zheng, J., Pu, H. and Zhang, L. (2011), "Analysis of excavation-induced responses of loaded pile foundations considering unloading effect", *Tunn. Undergr. Sp. Tech*., **26**(2), 320-335. https://doi.org/10.1016/j.tust.2010.11.003.

Zhang, L.M. and Ng, A.M.Y. (2005), "Probabilistic limiting tolerable displacements for serviceability limit state design of foundations", *Géotechnique*, **55**(2), 151-161. https://doi.org/10.1680/geot.2005.55.2.151.